

Design and Optimization of MEMS based AlN sensor for Acoustic Application

Mohini Sawane^{a,b}, Mahanth Prasad^{a,b*}, & Rajesh Kumar^c

^aCentral Electronics Engineering Research Institute, Pilani 333 031, India

^bAcademy of Scientific and Innovation Research (AcSIR), Ghaziabad 201 002, India

^cUniversity School of Basic & Applied Sciences, Guru Gobind Singh Indraprastha University, New Delhi 110 078, India

Received: 10 May 2023; Accepted: 30 May 2023

The market for MEMS sensors based on Aluminum Nitride (AlN) is developing because of AlN material's capacity to produce CMOS-compatible, highly reliable, and self-powered devices. Utilizing the COMSOL software tool, the sensors parameters are designed and optimized in accordance with the dimension and thickness of AlN thin film layer. The proposed design technique is applicable to any piezoelectric diaphragm-based acoustic sensors, regardless of the cavity and hole structures in the silicon or SOI (silicon on insulator) based substrate. The diaphragm consists fixed 25 μm Si layer and variable (0.5 μm to 2.5 μm) Al/AlN/Al layer. The AlN layer is sandwiched between top and bottom Aluminum electrodes of thickness 0.3 μm . The diaphragm area is varying from 1.75 mm x 1.75 mm to 3.5 mm x 3.5 mm. Prior to engaging in expensive fabrication methods, this work optimizes the AlN layer with regard to resonance frequency, deflection at the diaphragm's center, and sensor response. The simulated results demonstrate the trade-off between the diaphragm deflection at the center and a workable frequency range in accordance with the design parameters that were specified. For a frequency range of 0.5 kHz to 18 kHz, the device's optimal design has a simulated sensitivity of 2.5 $\mu\text{V}/\text{Pa}$ and at resonance the sensitivity is 200 $\mu\text{V}/\text{Pa}$.

Keywords: MEMS sensor, Piezoelectricity, AlN thin film, Design optimization

1 Introduction

In response to mechanical vibration, such as sound pressure, tension, or strain, AlN material has the ability to generate an internal electric field. This material property is called piezoelectric effect. They are self-generating devices that can run without an external power source. AlN films with controlled (low) residual stress and good piezoelectric response are qualities that are ideal for MEMS manufacturing¹. For the films to achieve high electromechanical coupling factor values, they must have a pure (00.2) orientation. Ionic bombardment is used to provide enough energy to the growing material in order to attain this state¹. A monolithic piezoelectric MEMS-CMOS microphone based on AlN is reported². The AlN and SiO₂ layers that make up the MEMS microphone's circular membrane are each 1 μm thick. The membrane radius, package dimensions, and electrode coverage have been tuned to 800 μm , 10 mm x 5 mm x 5 mm, and 15 %, respectively, to maximize the microphone bandwidth and limit the effects of acoustic package and parasitic, input buffer capacitance, and sensitivity. With a resonance frequency of 11.2 kHz, the integrated device

has an average off-resonance sensitivity² of 0.68 mV/Pa. For use in MEMS acoustic sensors³, the piezoelectric AlN layer was annealed at various temperatures to improve the piezoelectric characteristics. The proposed technique's procedure³ is easier to follow and more reliable. It fixes the flaws and restrictions of the prior method, making it safe to use in the production of MEMS acoustic sensors and similar technologies³. The AlN-based MEMS structure that was successfully constructed has a resonance frequency³ of 42.9 kHz. The previously suggested work covers a wide variety of topics related to the use of AlN as an actuation layer in MEMS, including its deposition conditions, precise interferometric device characterization, and the extraction of physical parameters⁴. Piezoelectric cantilever MEMS microphone was created using a FEA model⁵, and the performance was compared to the theoretical results. A strong correlation between the simulation and theoretical results are found after comparing them⁵. The MMOP platform enables designers to create optimal designs in less time with respectable confidence in the expected performance of the system⁵. For inertial sensors, such gyroscopes, where the actuation and sensing directions are firmly perpendicular, in-plane actuation is necessary⁶.

*Corresponding author (E-mail: mahanth.prasad@gmail.com)

High SPL levels between 120 and 160 dB can be tolerated by silicon diaphragms⁷ with a thickness of 25 μm . The piezoelectric-based acoustic sensor has the benefit over condenser-based ones because it does not require biasing, making it simpler and less expensive to manufacture⁷. The sensitivity thus obtained for the center and outer annular electrode patterns is 103 and 84 $\mu\text{v}/\text{Pa}$, respectively⁷. The piezoelectric AlN MEMS devices' full potential is unlocked by finite-element modelling (FEM) of the MEMS gyroscope with AlN thin films on vertical sidewalls. The half-fork MEMS gyroscope's FEM modelling of inertial sensing offers a considerable scaling advantage, and its output is competitive with another commercial angular rate sensors⁶. The COMSOL Multiphysics (COMSOL) FEM simulations enable the measurement of the angular rate sensitivity with the peak value of 1 mV/dps, demonstrating the potential of AlN sidewall structures in MEMS gyroscopes⁶. Due to their effectiveness in converting mechanical energy to electric charge and vice versa, MEMS-based piezoelectric sensors are used widely⁸. It is an increasingly growing technology since the fabrication process for MEMS-based devices has been optimized^{1,2}. But the manufacturing process is costly. Before beginning any expensive fabrication process, design optimization using a Multiphysics computing tool like COMSOL helps in understanding and evaluating device response. In order to produce the highest possible sensor response, this work suggests in-depth research into various sensor design aspects. Square shaped AlN deposited diaphragm (Silicon) is considered to produce maximal deflection at the center for acoustic applications.

2 Materials and Methods

The COMSOL Multiphysics tool is used to design the proposed device. Prior to using MEMS fabrication processes, the simulated results demonstrate the relationship between resonance frequency, deflection, and output response. Material selection, geometry selection, and diaphragm optimization are the three key factors to consider when designing AlN-based acoustic sensors. These factors are covered in more detail in the following sections.

2.1 Material selection

The applied force can cause the piezoelectric to produce an electric charge. This physical characteristic of piezoelectric material allows for the use of piezoelectric materials in self-powered sensor

categories. The most popular piezoelectric materials using MEMS-based fabrication technologies are ZnO, AlN, and PZT. Thin film ZnO and AlN are suitable piezoelectric materials for CMOS based fabrication processes. The Table 1 provides information on the characteristics⁹ of piezoelectric materials, including density, piezoelectric constant, dielectric constant, Young's modulus, quality factor, electromechanical coupling factor, and loss tangent. Using non-approximated equations that can account for multiple film stacking, the parameters of AlN-driven multilayered cantilevers, including Young's modulus related to the (0 0 2) orientation of the crystallites, residual thin film stresses, thermal expansion coefficient, and piezoelectric coefficient d_{31} , have been calculated⁴. The properties of the well-oriented thin films are similar to those of the bulk material⁴. The significant influence of AlN as a seed layer on the crystalline quality, piezoelectric characteristics, and graining of $\text{Y}_{0.15}\text{Al}_{0.85}\text{N}$ thin films are studied¹⁰. Furthermore, $\text{Y}_{0.15}\text{Al}_{0.85}\text{N}$ exhibits great stability up to 800 °C with just a minor loss in oxidation resistance in a 100% oxygen environment as compared to pure AlN, as shown by high-temperature in situ XRD tests. The $\text{Y}_{0.15}\text{Al}_{0.85}\text{N}$ thin film with the seed layer has a piezoelectric constant of d_{33} of 7.85 pC N⁻¹ and a Young's modulus of 249 ± 5.66 GPa. AlN and even scandium alloyed with AlN as a functional material in upcoming silicon MEMS applications, such as sensors, actuators, or high-frequency filter elements, could very well be replaced by $\text{Y}_{0.15}\text{Al}_{0.85}\text{N}$ thin films produced on an AlN seed layer¹⁰. AlN is a material with low values for the piezoelectric coefficients but high values for the young's modulus, band gap, dielectric strength, resistance, thermal conductivity, and acoustic velocities. It is a very adaptable material, both in bulk and thin-film forms, and is ideal for a number of applications due to its comprehensive physical and chemical properties¹¹. Despite the widespread use of AlN in RF acoustic filters and

Table 1 — Properties of piezoelectric materials

Materials / Parameters	PZT	AlN	ZnO
Density (Kg/m^3)	7.6	3260	5660
Piezoelectric constant d_{33} (pC/N)	223	5	12.4
Piezoelectric constant d_{31} (pC/N)	33	-5.43	-5
Dielectric Constant	1300	8.5	10.9
Young's Modulus (GPa)	98	310	210
Quality factor	75	2490	1770
Electromechanical coupling factor	35	8	1.7
$\tan \delta$	0.03	0.003	0.1

transducer applications in MEMS, improved electromechanical coupling and system performance can still be attained by improving the piezoelectric coefficients¹². The doping has been done with scandium, boron, or magnesium, but additional options might be possible and necessitate more investigation at the material level¹³. In order to ensure selective/controlled etching, removal of the etching by-products, avoid contaminating process equipment, and maintain compatibility with the underlying CMOS device, etching procedures will need to be tuned for these doped materials¹⁴⁻²⁵. For AlN to be successful in the past, CMOS-compatible thin-film deposition by magnetron sputtering was essential. The adoption of alternative production techniques, however, as well as the reduction of carbon emissions, are the difficulties for the twenty-first century¹¹. The conventional IC and MEMS microfabrication procedures, which are energy-intensive and primarily reliant on subtractive operations, are somewhat incompatible with these objectives and environmental challenges^{11,12-25}. Thus, it is necessary to research localized deposition techniques in order to avoid the lithographic and etching processes. It is possible to use powder and solution deposition processes, such as binder jetting and inkjet printing, for some applications that just need the outstanding dielectric properties of AlN¹¹. However, in the future, it will be necessary to create dependable additive manufacturing techniques for the production of piezoelectric AlN devices, which call for well-oriented crystalline layers. Additionally, it is desirable to fabricate AlN transducers and integrated systems on polymer and flexible substrates for some applications, even though these materials reveal challenges in terms of fabrication, layer bond strength, interplay between interface layer, and device durability and reliability when the substrate is strained. Only time will tell how many further application opportunities aluminium nitride as a MEMS material will meet, whether for standalone devices or integration with CMOS¹¹. In a moist environment, AlN thin film-based MEMS sensors are more reliable than ZnO. Hence, in this work for MEMS and CMOS technology-based acoustic devices, AlN is the excellent material to use.

2.2 Geometry selection

The most popular piezoelectric-based MEMS geometries are circular and square in shape. Depending on the intended function, both the circular

and square shapes have advantages. The square diaphragm is taken into consideration for the proposed work. The proposed design makes use of a square diaphragm that is clamped on all sides and free on the top and bottom surfaces. The center of a square diaphragm experiences the most deflection, which is suitable for specialized acoustic sensor applications. Each side close to its respective clamping experiences the highest level of stress. The deflection of diaphragm⁸ is shown in Equation (1).

$$y = \frac{Pa^4(1-\nu^2)}{4.2Eh^3} \quad \dots (1)$$

Where, y = deflection of diaphragm; P = applied pressure (Pa); a = half of diaphragm length; ν = Poisson ratio; E = young modulus; h = thickness. This is the first order linear equation is considered for proposed design.

2.3 Diaphragm optimization

Before commencing sensor fabrication, the one of the most crucial phases is designing and optimizing AlN layer thickness, and placement on cavity. For variable sizes and AlN layer thicknesses, the silicon diaphragm thickness is constant and taken as 25 μm . Later in the silicon thickness is also optimized and reduced to 5 μm . The width and depth of a microtunnel are fixed for all dimensional permutation.

The microtunnel has a depth of 35 μm and a width of 100 μm . The length and effective length of microtunnel is changes with every different dimension considered and it depends on cavity dimension. The aluminium electrode is considered of 0.3 μm fixed thickness and area is varying as per the AlN area. Cavity depth 375 μm fixed for all explored geometry. Area of the cavity changes with change in area of AlN diaphragm. A MEMS-based micromachining method is considered for designing thin film AlN based acoustic sensors. In order to achieve the highest feasible sensitivity with the broadest possible operational frequency range, the proposed work aims to optimize the AlN layer and its electrode in terms of surface area and thickness. The Fig. 1 Illustrates the designed three-dimensional device module in COMSOL software. The microtunnel and cavity structures are formed in most of the acoustic sensor for pressure compensation. The device safety is ensured by this pressure compensation technique. The diaphragm illustrated in Fig. 2 is consists of silicon, aluminium (Al) bottom electrode layer, AlN layer as piezoelectric layer and top Aluminium layer as top electrode.

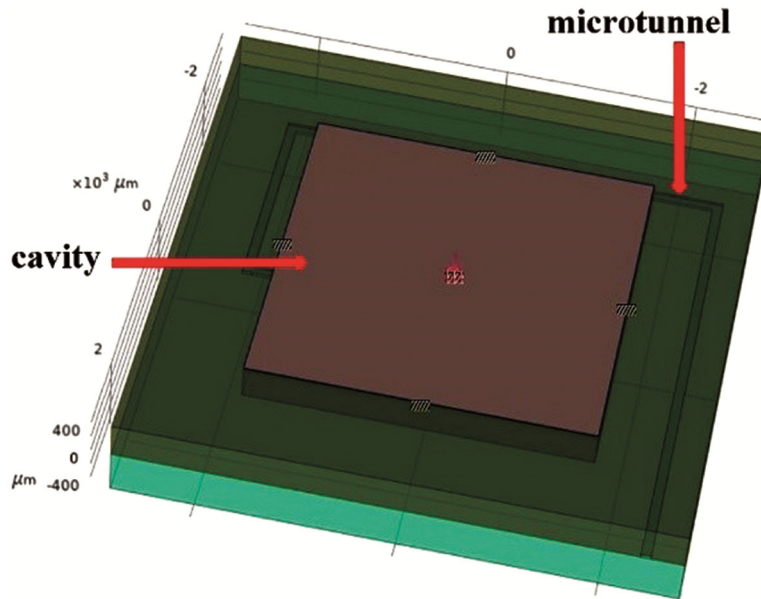


Fig. 1 — Designed 3D model with the help of COMSOL software.

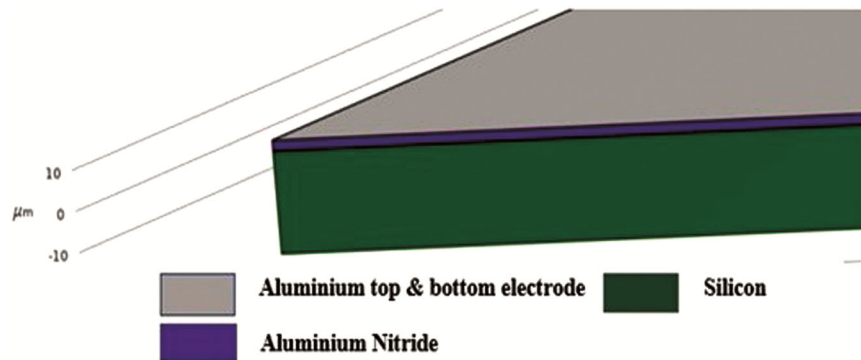


Fig. 2 — Designed 3D large view of diaphragm (Si/Al/AlN/Al).

3 Results and Discussion

Resonance frequency is one of the most crucial output response factors for piezoelectric-based acoustic sensors. Some transducers, including energy harvesters and FBAR, work at resonance frequencies. Flat frequency response is necessary for some acoustic sensors, such as hydrophones and microphones. For devices to have a wider range of functions, especially in the case of microphones, a high resonance frequency value is preferred. One fourth of the resonance frequency is a general rule for flat response. The theoretical flat response limit of the computed resonance frequency in Fig. 3 is 34 kHz because it is 136 kHz. Additionally, substrate structure is crucial in determining the lower cutoff frequency for a flat response. In flat response-based acoustic devices, the lower cut-off frequency is estimated using the following equation⁸.

$$f_L = \frac{1}{2\pi R_a C_{cav}} \quad \dots (2)$$

$$R_a = \frac{128\mu_{air} L_{eff}}{\pi D_{vent}^4} \quad \dots (2a)$$

$$C_{cav} = \frac{V_{cav}}{C^2 \rho_{air}} \quad \dots (2b)$$

Where f_L = lower cut-off frequency; R_a = tunnel resistance; C_{cav} = cavity compliance; D_{vent} = tunnel diameter; μ_{air} = viscosity of air; L_{eff} = effective length of tunnel; C = speed of sound; ρ_{air} = air density. The Figure 3 shows the simulated resonance frequency at 136 kHz for an AlN layer with a thickness of 1.5 μm , a silicon layer of 25 μm , and 1.75 mm x 1.75 mm diaphragm area. As the length of the square diaphragm is increased, the simulation result in Fig. 4 demonstrates that the resonance frequency reduces. For AlN thickness, which ranges

from 0.5 μm to 2.5 μm , the trend is also downward. This leads to the conclusion that as diaphragm length and ultimately area increase, resonance frequency decreases. The area for simulation is considered as 1.75 mm x 1.75 mm and that means length of square diaphragm is 1.75 mm. The Fig. 5 shows the

deflection versus AIN thickness plot at constant area of 1.75 mm x 1.75 mm. The maximum deflection is occurred for 1.5 μm AIN thickness. When the diaphragm is optimized, the optimal dimensions are determined to be at 1.5 μm of AIN thickness and 1.75 mm x 1.75 mm of diaphragm area.

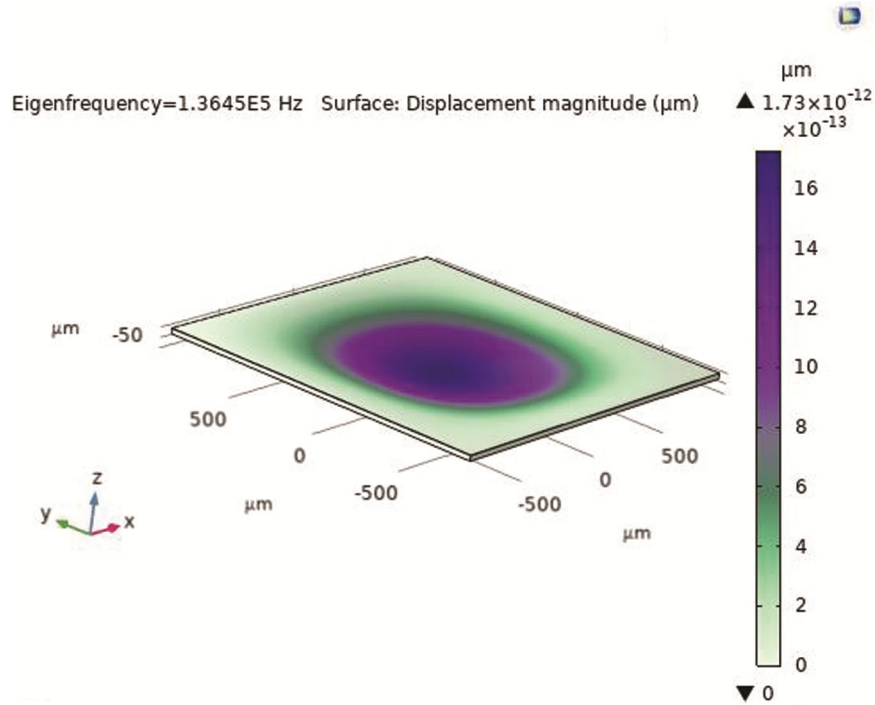


Fig. 3 — Simulated result for AIN thickness of 1.5 μm , silicon diaphragm is of 25 μm and diaphragm area is 1.75 mm x 1.75 mm. The maximum deflection of $1.73 \times 10^{-12} \mu\text{m}$ achieved at 136 kHz resonance frequency.

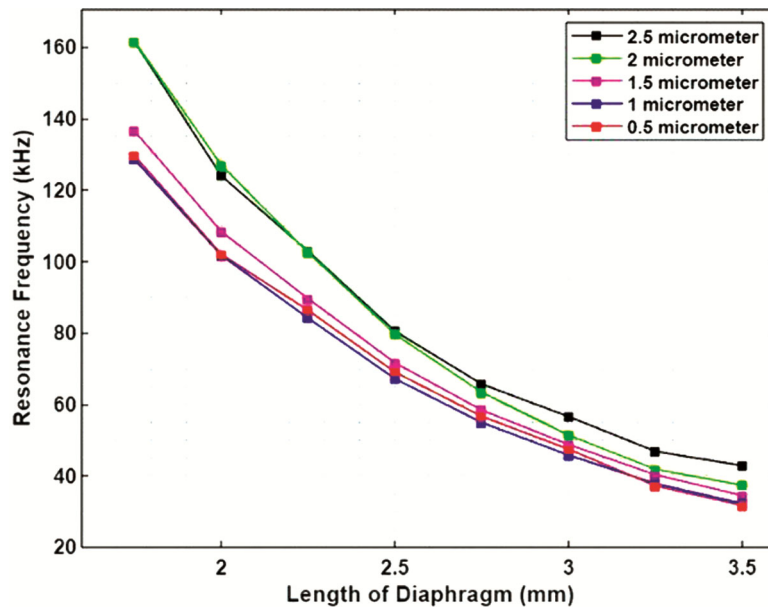


Fig. 4 — Comparing resonance frequency versus length of square diaphragm for AIN thickness ranging from 0.5 μm to 2.5 μm with respect to length ranging from 1.75 mm to 3.5 mm for each thickness of AIN.

The Si thickness is taken as 25 μm but it causes less deflection. Hence the diaphragm optimized again with Si layer thickness of 5 μm , AlN thickness of 1.5 μm and area of diaphragm is 1.75 mm x 1.75 mm. Simulated results for final optimized diaphragm show that deflection is increases as the overall diaphragm thickness reduced by making Si of 5 μm . When

compared to 136 kHz resonance frequency for 25 μm of Si with the same other parameters, the simulated resonance frequency for 5 μm thick Si is approximately 58 kHz, which is lower. The Fig. 6 show the simulated sensitivity of proposed device after optimization and it is averaged around 2.5 $\mu\text{V}/\text{Pa}$ at flat frequency range is from 5 Hz to 18 kHz.

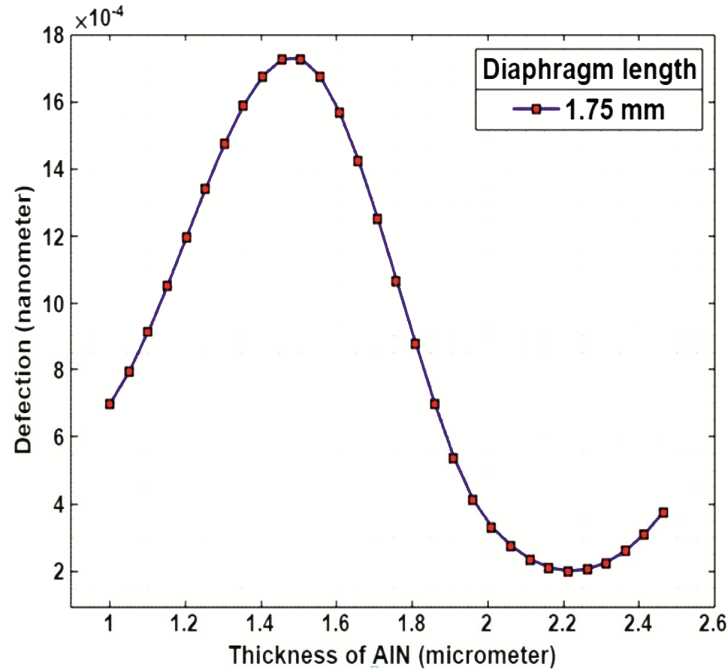


Fig. 5 — Deflection versus AlN thickness at constant area of 1.75 mm x 1.75 mm. The maximum deflection occurred at 1.5 μm AlN thickness.

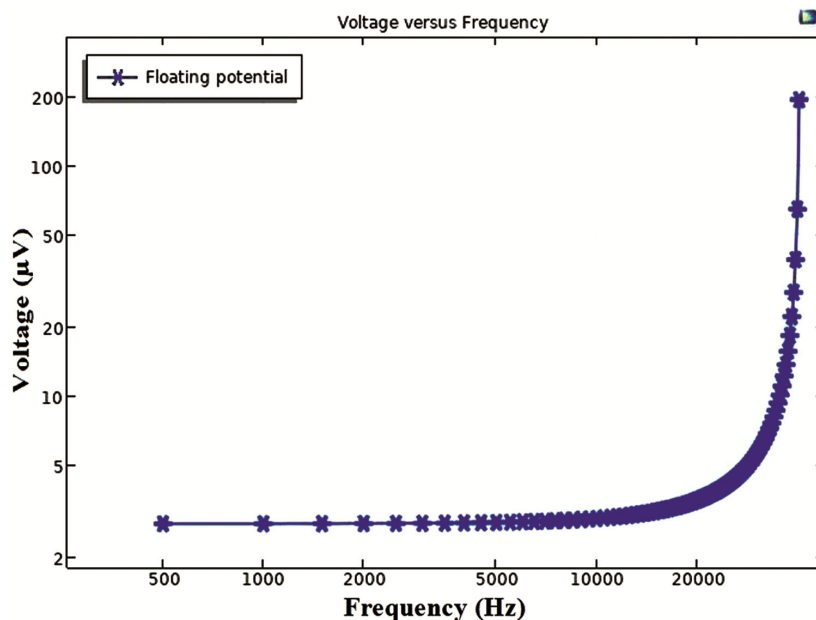


Fig. 6 — Sensitivity and frequency range of proposed design after optimization. The flat response sensitivity is 2.5 $\mu\text{V}/\text{Pa}$ for frequency range of 500 Hz to 18 kHz. The sensitivity at resonance is 200 $\mu\text{V}/\text{Pa}$.

4 Conclusion

One crucial factor in determining a device's operational frequency range is resonance frequency. As the diaphragm's thickness increases, the resonance frequency decreases. Due to the diaphragm's fixed 25 μm Si layer and variable AlN layer (ranging from 0.5 μm to 2.5 μm). It is determined that the proposed design is best suited for 1.5 μm AlN thickness. The simulated resonance frequency is 136 kHz for optimized diaphragm at 25 μm of Si thickness. Resonance frequency is reduced further if Si thickness is reduced to 5 μm but it eventually increases the deflection. This increased deflection increases the sensitivity of optimized device further. The thickness and area of the diaphragm play a major role in how much it deflects. Out of all the variations mentioned, the diaphragm with a 1.75 mm x 1.75 mm area gives the most optimal outcomes with 1.5 μm of AlN thickness. Before starting fabrication of device, the diaphragm's optimization provided a comprehensive grasp of parameter dependency. The sensitivity of the designed sensor is improved through diaphragm optimization and it is 2.5 $\mu\text{V}/\text{Pa}$ for frequency range from 0.5 kHz to 18 kHz without amplification. The simulated resonance frequency is 58 kHz, and the optimized device's sensitivity is 200 $\mu\text{V}/\text{Pa}$.

Acknowledgment

The authors would like to thank the Director, CSIR-CEERI, Pilani, for encouragement and guidance.

References

- Iborra Enrique, Olivares Jimena, Clement Marta, Vergara Luize, Sanz-Hervás A, Sangrador Jesus, *Sens Actuator A Phys*, 115 (2004) 501.
- J. Segovia-Fernandez *et al.*, Monolithic piezoelectric Aluminum Nitride MEMS-CMOS microphone, 19th International Conference on Solid-State Sensors, Actuators and Microsystems (TRANSDUCERS), 414 (2017).
- Mahanth Prasad, Rajesh Kumar, *Vacuum*, 157 (2018) 349.
- Alexandru Andrei, Katarzyna Krupa, Michal Jozwik, Patrick Delobelle, Laurent Hirsinger, Christophe Gorecki, Lukasz Nieradko, Cathy Meunier, *Sens Actuator A Phys*, 141 2 (2008) 565.
- Ahmed Fawzy, Ahmed Magdy, Aya Hossam, *Alex Eng J*, 61 4 (2022) 3175.
- Artem Gabrelian, Glenn Ross, Kristina Bepalova, Mervi Paulasto-Kröckel, *Mat Today Commun*, 33 (2022) 104522.
- Arya, D.S., Kumar, S., Prasad, M., Singh, P., Tripathi, C.C., *The Physics of Semiconductor Devices. IWPSD* (2019).
- M. Prasad, Aditi and V. K. Khanna, *IEEE Trans Ind Electron*, 693 (2022) 3142.
- Mohini Sawane, Mahanth Prasad, *Mater Sci Semicond*, 158 (2023) 107324.
- Pandit S, Schneider M, Berger C, Schwarz S, Schmid U, *Adv Electron Mater* (2022) 2200789.
- R. M. R. Pinto, V. Gund, R. A. Dias, K. K. Nagaraja and K. B. Vinayakumar, *J Microelectromech*, 314 (2022) 500.
- James R, Pilloux Y, & Hegde H, *J Physics: Conf Ser*, 1407 (2019) 012083.
- Nie R, Shao S, Luo Z, Kang X, Wu T, *Micromachines*, (2022) 1629.
- Uehara Masato, Shigemoto Hokuto, Fujio Yuki, Nagase Toshimi, Aida Yasuhiro, Umeda Keiichi, Akiyama Morito, *Appl Phys Lett*, (2017).
- Lei H, Wen Q, Yu F, Li D, Shang Z, Huang J, Wen Z, *J Micromech Microeng*, (2018) 115012.
- Meinel K, Stoeckel C, Melzer M, Zimmermann S, Forke R, Hiller K, Otto T, *IEEE SENS J*, (2019) 1.
- Schneider, M., Pfusterschmied, G., Patocka, F. *et al*, *Elektrotech. Inftech*, 137 (2020) 121.
- Ababneh M, Alsumady H, Seidel T, Manzanique J, Hernando-García, J.L. Sánchez-Rojas, A Bittner, U. Schmid, *Appl Surf Sci*, 259 (2012) 59.
- Atul Vir Singh, Sudhir Chandra, A.K. Srivastava, B.R. Chakroborty, G. Sehgal, M.K. Dalai, G. Bose, *Appl Surf Sci*, 257 22 (2011) 9568.
- Iqbal A, Mohd-Yasin F, *Sensors*. (2018) 1797.
- Lueng C, Chan H, Surya Charles, Choy C, *J Appl Phys*, 88 (2000) 5360.
- Calabrese E, Fowler W B, *Condens Matter*, 186 (1978) 2888.
- Zang Y, Li L, Ren Z, Cao L, and Zhang Y, *Surf Interface Anal*, 48 (2016) 1029.
- Tarumi R, Nakamura K, Ogi H, Hirao M, *J Appl Phys*, 102 11 (2007) 113508.
- Hassan YSavaria and M Sawan, *IEEE Access*, 6 (2018) 78790.